

**EXTENDED DYNAMIC RANGE MICRO-COMPUTED TOMOGRAPHY OF METORITES USING A BIOMEDICAL SCANNER.** D.R. Edey<sup>1</sup>, P.J.A. McCausland<sup>1</sup>, D.W. Holdsworth<sup>2</sup>, and R.L. Flemming<sup>1</sup>, <sup>1</sup>Dept. of Earth Sciences, U. of Western Ontario, London, ON, N6A 5B7, <sup>2</sup>Robarts Research Institute, U. of Western Ontario, London, ON, N6A 3K9.

**Introduction:** Micro-computed tomography (micro-CT) can be a powerful tool for analysis of meteorite samples. The ability to visualize internal structure non-destructively has proven to be an effective way of examining samples that are too rare or valuable to cut, or as a means of primary investigation before cutting begins [1,2]. It also can act as an archival medium in which samples can be digitally preserved prior to modification or destruction.

There is a large installed base of biomedical micro-CT scanners worldwide. These devices can provide high spatial resolution on small specimens but operate at lower x-ray voltages, leading to potential image artifacts. Artifacts due to dense materials can lead to incorrect signal levels in the interior of specimens, confounding analysis, and can also lead to streak artifacts that obscure details both on the interior and exterior of the specimens [3]. The major source of these errors includes beam hardening (due to the preferential removal of low-energy photons in a polyenergetic spectrum), scatter, and under-ranging (inadequate dynamic range), manifested as inadequate recording of extremely dark signals [4].

Using empirical data gathered from scanning an in-house designed calibration phantom it is possible to reduce or remove the offending artifacts from previously collected data, as long as the original projections have been preserved [5,6].

Two meteorites have been chosen for this study, NWA 5480 (Figure 2) is an olivine diogenite and Ozoona (Figure 3) is a weathered H chondrite. These were chosen to test the ability of the correction algorithm to restore largely uniform matrix density with some higher density spot and fracture-filling features.

**Methods:** All meteorite data was collected previously on an eXplore speCZT (speCZT) [GE Healthcare] at peak energies of 80 to 110 kVp [7]. For each sample, 900 projections were collected in a single



**Figure 1: Calibration Phantom, consists of 8 aluminum disks in an alternating step configuration.**

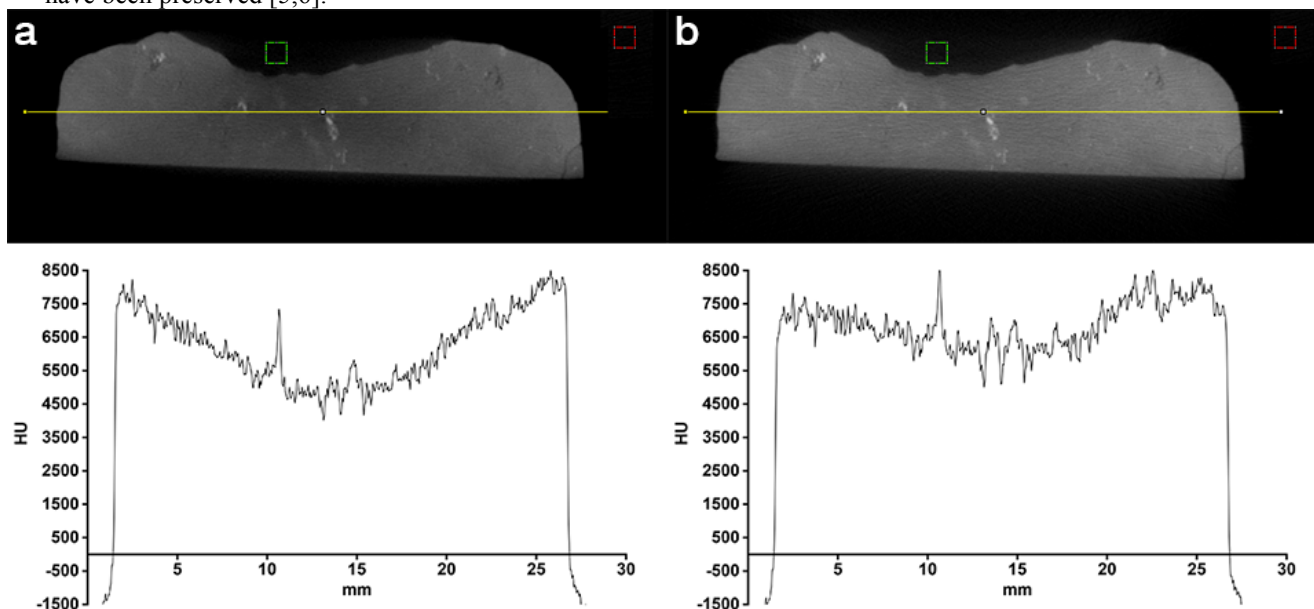


**Figure 2: The same micro-CT cross-section of NWA 5480 before (a) and after (b) correction. The yellow lines denote the cross section location and the square ROIs are 20 x 20 voxels used for streaking measurements.**

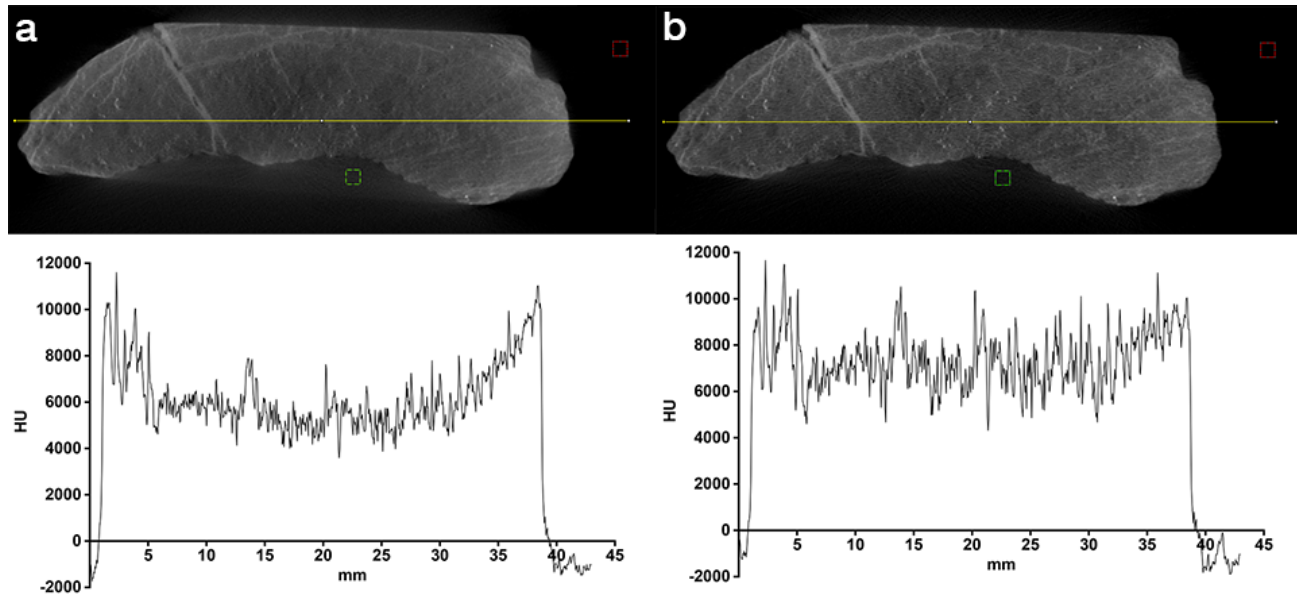


**Figure 3: Ozona - The same micro-CT cross-section of Ozona before (a) and after (b) correction. The yellow lines denotes the cross section location and the square ROIs are 20 x 20 voxels used for streaking measurements.**

360° rotation with a 16 millisecond exposure per projection. This allows for a full scan to be performed in 5 minutes.

For this study a calibration phantom was also scanned. This aluminum (6061-T6) calibrator (Figure 1) has 8 aluminum disks ranging from 4.15 to 59.25 mm in diameter and stacked in a configuration designed to most accurately mimic the scatter profile of irregular shaped objects.

Calibrator scan data was collected at a peak energy of 90 kVp with all other collection parameters kept the same. The data produced by the calibrator contains information of the non-linearity of the system. This non-linearity in response to attenuation is then modeled using an inverse decay formula to re-linearize each projection on a pixel-by-pixel basis.

After re-linearization, the projections are reconstructed into CT volumes with an isotropic spatial resolution of 25  $\mu\text{m}$  using software packaged with the micro-CT scanner.

**Discussion:** After reconstruction the effects of the re-linearization can be seen in the CT volumes.

**Cupping:** Line profiles seen throughout the volumes pre-correction (Figure 2a, 3a) illustrate the cupping artifact where the center of the specimens show an artificially low density in Hounsfield Units (HU) whereas after correction (Figure 2b, 3b) the line profiles are much more uniform and the centers of the objects appear closer in density to their edges.

**Streaking:** Streaking between two sections of rock can easily be seen in the sections of air shielded by the rest of the sample. Regions of interest (ROIs) were placed in these regions (2,3 outlined in green) and their

	NWA 5480 (2)		Ozona (3)	
	Control (HU)	ROI (HU)	Control (HU)	ROI (HU)
Precorrection	-1108.8	-606.1	-1195.5	-410.2
Postcorrection	-1058.0	-892.6	-1127.3	-765.2

**Table 1: HU measurements of shown ROIs.**

average value in HU was compared to that of a section of unperturbed (control) air (2,3 outlined in red) (Table 1). The streaking is significantly reduced within the shielded sections, and air values were improved by over 50% of uncorrected values.

**Summary:** The use of empirical data collected from a calibration phantom makes the correction of artifacts seen in previously scanned specimens possible. This correction re-linearizes the transmission data of projections on a pixel-by-pixel basis, reducing cupping in the interior of the object as well as streaking. In summation, we show a correction method that can be applied retrospectively to further increase the usefulness of biomedical micro-CT to the geological sciences, in particular, the examination of interior features of meteorite samples.

**References:** [1] Arnold, J.R. et al. (1983) *Science* 219, 383-384. [2] Friedrich, J. M. (2008) *Comp. Geosci.* 34, 1926-1935. [3] Brooks, R.A. and Di Chiro, G. (1976) *Phys. Med. Biol.* 21, 390-398. [4] Ketcham, Richard A. and Carlson, William D. (2001) *Comp. Geosci.* 27, 381-400. [5] Chen, C.Y. et al. (2001) *J. Dig. Imag.* 14, 54-61. [6] Herman, G.T. (1979) *Phys. Med. Biol.* 24, 81. [7] McCausland, P.J.A. et al (2010) *LPSC XLI Abstract #2584.*